CHIN. PHYS. LETT. Vol. 32, No. 8 (2015) 084201

Tunable, High-Order Harmonically Mode-Locked All-Normal-Dispersion Ytterbium Fiber Laser *

LV Zhi-Guo(吕志国)[1], TENG Hao(滕浩)[2**], WANG Li-Na(王立娜)[2], WANG Rui(王睿)[2], WEI Zhi-Yi(魏志义)[1,2**]

[1]*School of Physics and Optoelectronic Engineering, Xidian University, Xi'an 710071*
[2]*Beijing National Laboratory for Condensed Matter Physics, Institute of Physics, Chinese Academy of Sciences, Beijing 100190*

(Received 7 April 2015)

We report the generation of passively tunable high peak signal-to-noise ratio harmonic mode-locked (HML) all-normal-dispersion Yb-doped fiber laser with a single birefringent filter in a ring cavity configuration. The highest fourth harmonic of the fundamental mode-locked frequency at a repetition rate of 88 MHz is obtained. The pulses are compressed to 627 fs by using an external grating-pair compressor. For the fourth HML output, the peak signal-to-noise ratio of the rf is 73 dB and the average power is as high as 110 mW with the pump power of 500 mW. Soliton bunches which contain multipulses are also observed in the weak mode-locked regime of the HML, and the separation between interpulses in a dissipative soliton bunch can be controlled by adjustment of the waveplates and spectral filter in the cavity.

PACS: 42.55.Px, 42.55.Wd, 42.55.Xi DOI: 10.1088/0256-307X/32/8/084201

Mode-locked fiber lasers have attracted significant interest for their potential advantages in compact design and reduced alignment sensitivity as well as excellent beam quality. As an excellent laser source, the passively mode-locked fiber laser opens a way to realize ultrahigh-repetition-rate pulse train with low timing jitter, which has found wide applications in microfabrication, optical communications, optical metrology, and optical frequency combs.[1] Secondly, with the emergence of the harmonic mode-locked (HML) technology,[2] the repetition rate of the passively mode-locked fiber laser was greatly increased, and up to gigahertz (GHz) repetition rate has been realized in Er-doped fiber lasers and/or in Yb-doped fiber lasers with anomalous dispersion.[3–7]

As a novel paradigm for the generation of ultrashort pulses, chirped pulse spectral filtering based ANDi fiber lasers have been widely studied due to the advantage of the removal of the anomalous-dispersion segment, which provides a possibility for realization of higher energy pulses directly from the fiber oscillator. However, due to the great tolerance of the nonlinear phase shift in the ANDi fiber laser, it is relatively difficult to realize high-order pulse splitting similar to the soliton fiber laser. For example, in 2011, Yang *et al.* reported passive second order HML in ANDi fiber laser with pulse duration of 14.6 ps assuming a sech^2-pulse shape.[8] Recently, Wang *et al.* achieved a 99.6 MHz second order HML ytterbium fiber laser with direct output pulse duration of 5 ps. Gao *et al.* realized the fourth-ordered HML ANDi fiber laser with a super-mode-suppression ratio lower than 55 dB.[9,10] The highest harmonic order reported in the ANDi fiber laser to date has been 14th HML output with 2.53 MHz fundamental repetition rate and a cascade long period fiber grating as spectral filter for modulations of the amplitude and spectrum. However, due to the longer fiber employed in the cavity and the instability introduced by fiber, the pulse duration was restricted to 1.3 ns and the super-mode-suppression ratio was 23 dB due to the sensitivity of the birefringence in an optical fiber to the surrounding's temperature.[11]

In this Letter, we report a nonlinear polarization evolution-based stable tunable high peak signal-to-noise ratio HML ANDi Yb fiber laser at 1046 nm, which generates the highest fourth HML with 73 dB peak signal-to-noise ratio at a repetition rate of 88 MHz and a direct (uncompressed) pulse duration of 15.5 ps. Compared with the previous reports in high-order HML ANDi fiber lasers, significant improvement is obtained in peak signal-to-noise ratio. After compression, pulses with duration of 627 fs are obtained with a sech^2 fit. We also experimentally study the evolution of the separation of the interpulses in a dissipative soliton bunch in the process of the realization of the harmonic mode locking. It also exhibits a 1.25 nJ of pulse energy at the fourth HML output and the obtained high peak signal-to-noise ratio also shows the excellent environmental stability.

Figure 1 shows the schematic diagram of our passive harmonically mode-locked ANDi Yb-doped fiber laser. It consists of a 976 nm laser diode (LD) with a maximum pump power of 500 mW, a 980/1030 nm wavelength division multiplexer (WDM), a 40 cm of Yb-doped fiber (YDF), an optical isolator with an effective operating range from 1044 to 1084 nm, a polarization controller (PC) consisting of two quarter-

*Supported by the National Key Technology R&D Program of the Ministry of Science and Technology under Grant No 2012BAC23B03, the National Key Basic Research Program of China under Grant No 2013CB922401, and the National Natural Science Foundation of China under Grants No 11474002.

**Corresponding author. Email: hteng@iphy.ac.cn; zywei@iphy.ac.cn

© 2015 Chinese Physical Society and IOP Publishing Ltd

waveplates and one half-waveplate, polarizing beam splitters (PBS), a pair of high power fiber collimator at a central wavelength of 1040 nm, a birefringent plate with a thickness of 7.5 mm, and an optical coupler with 50% output. The other single-mode fibers used in the oscillator are 8.5 m HI 1060 with an estimated normal 22 fs^2/mm dispersion coefficient. The overall cavity length of the oscillator is approximately 9 m corresponding to a round-trip time of 45.45 ns and the total dispersion introduced into the cavity is estimated to be 0.2 ps^2. The pump laser from 976 nm LD is coupled into the YDF through the WDM in a forward pump configuration and the generated laser propagates unidirectionally in the ring cavity due to the confinement of the isolator. The birefringent plate inserted between polarizers at Brewster angle constitutes a narrow band spectral filter and its actual action is to chirp the pulses in spectral and temporal regime to introduce pulse-shaping mechanism so as to initiate mode-locking. The mode-locked output laser pulses are detected by a fast photo-diode and recorded with an oscilloscope (DPO 2024B), an optical spectrum analyzer (Yokogawa AQ6370), and a frequency spectrum analyzer (Agilent E4407B).

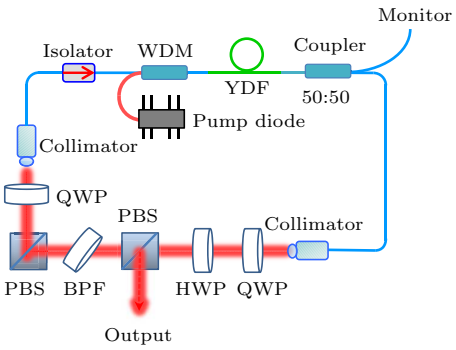

Fig. 1. Schematic diagram of the ANDi fiber laser. PBS: polarization beam splitter; QWP (HWP): quarter- (half-) waveplate; BPF: birefringent filter; WDM: wavelength division multiplexer.

Self-starting fundamental wave mode-locking is firstly realized by carefully adjusting the PC under a full pump power. The mode-locked pulse train on oscilloscope and the rf spectrum are shown in Fig. 2, where the repetition rate of fundamental pulses is 22 MHz.

Based on the stable fundamental mode-locking achieved, the mode-locked pulses train are gradually split into soliton bunches which contain two or more interpulses by slight adjustment of the orientations of the waveplates and birefringence filter without changing the pump power. Furthermore, the time interval of the interpulses in a soliton bunch can be experimentally controlled by adjusting the waveplates in the fiber laser. As solitons with equal amplitude are distributed periodically, thus the corresponding repetition frequency is equal to a multiple of the resonator round-trip repetition rate, the HML state is established. The corresponding dynamic evolvement of the second order HML is shown in Fig. 3.

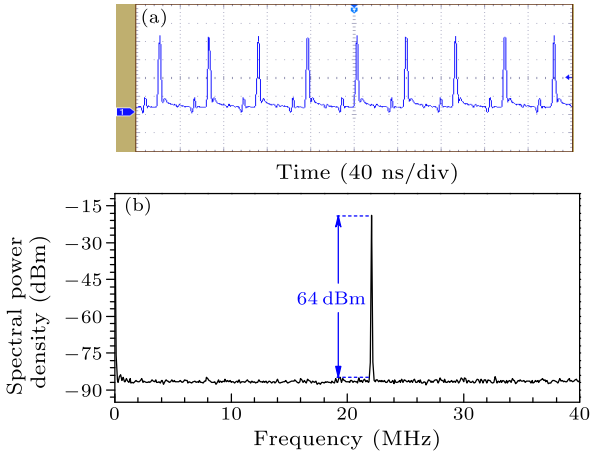

Fig. 2. (a) Pulse train on an oscilloscope; (b) the rf spectrum with 1 kHz resolution.

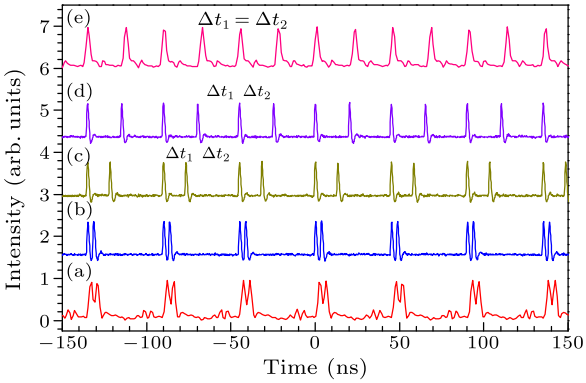

Fig. 3. Evolvement of the second order HML: (a) pulses splitting; (b) dual-pulse soliton bunch with equal amplitude; (c) dual-pulse soliton bunch with $\Delta t_1 = 13.31$ ns pulse separation, $\Delta t_2 = 32.14$ ns; (d) dual-pulse soliton bunch with $\Delta t_1 = 20.25$ ns pulse separation, $\Delta t_2 = 25.20$ ns; (e) second HML pulses, $\Delta t_1 = \Delta t_2 = 22.72$ ns.

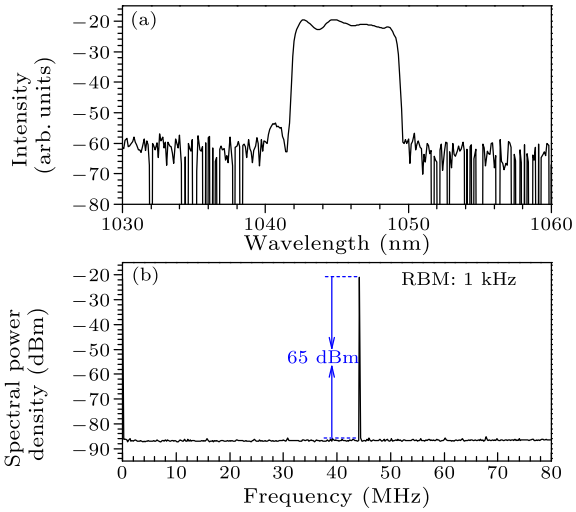

Fig. 4. Second order HML results at the wavelength of 1046 nm. (a) Optical spectrum measured at the output port of the PBS. (b) The rf spectrum with 1 kHz resolution.

Figure 4 shows the spectrum of the second order HML on a logarithmic scale with a 3 dB bandwidth of

6.5 nm and the rf spectrum.

The rf spectrum in Fig. 4(b) shows a high peak-to-pedestal extinction (∼65 dB) for the second order HML operation which indicates high stability. In addition, with continuous fine adjustment of the waveplates assisted with the rotation of the optical axis of the uniaxial birefringent filter, the higher-order harmonic mode-locked state could also be realized. The corresponding dynamic evolvements of the third and fourth-order HML are also shown in Figs. 5 and 6.

Figure 7 shows the spectra of the high-order HML on a logarithmic scale. For the third-order HML, the 3 dB bandwidth (8.6 nm) is slightly wider than that in fourth HML (7 nm).

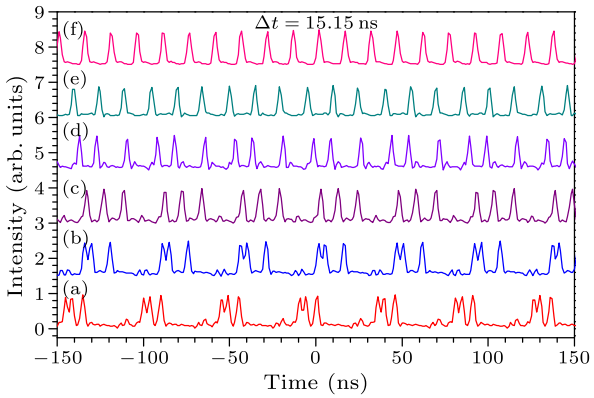

Fig. 5. Evolvement process on the formation of the third order HML: (a) pulse splitting (b) triple-pulse soliton bunch with one separated pulse; (c) triple-pulse soliton bunch with equal amplitude; (d) triple-pulse soliton bunch with hybrid pulse separations; (e) transition state before harmonic pulse formation; and (f) stable third HML pulses.

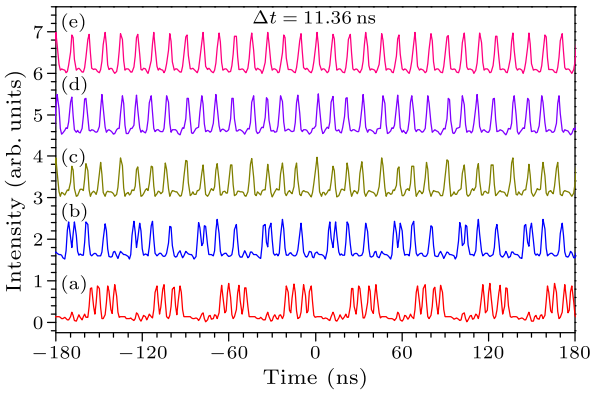

Fig. 6. Evolutionary process on the formation of the fourth order HML: (a) quadruple-pulse soliton bunch; (b) quadruple-pulse soliton bunch with two separated pulses; (c) quadruple-pulse soliton bunch with unequal amplitude; (d) transition state before harmonic pulse formation with four pulses coexisting in a bunch, but the separation between the pulses is not consistent; and (e) stationary distribution in stable fourth HML.

For third and fourth HMLs, the fundamental frequencies are 66 and 88 MHz, respectively, as shown in Figs. 8(a) and 8(b). The rf spectra in Fig. 8 show high signal-to-noise ratio (69 and 73 dB for third and fourth HMLs, respectively, at a resolution bandwidth of 1 kHz), which indicates high stability during mode-locking operation.

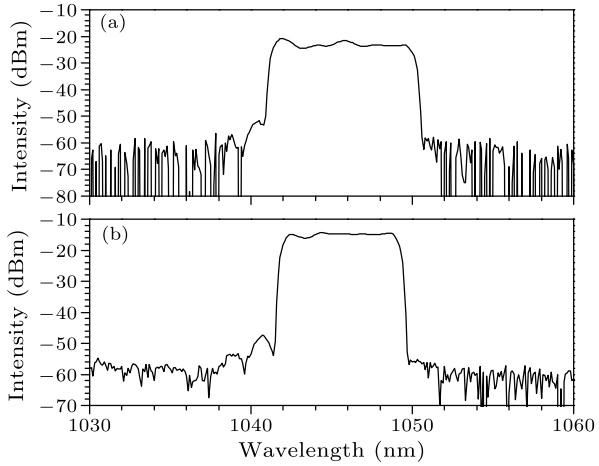

Fig. 7. HML spectra at the output port of the PBS. (a) Optical spectrum of the third order HML. (b) Optical spectrum of the fourth order HML.

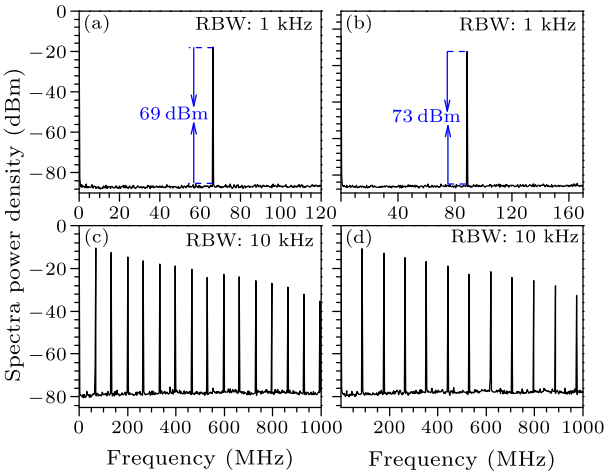

Fig. 8. (a) The rf spectrum of the third HML pulses for the 120 MHz scanning range with 1 kHz resolution. (b) The rf spectrum of the fourth harmonic at 88 MHz with 170 MHz span. (c) The rf spectrum at the third harmonic for the 1 GHz scanning range with 10 kHz resolution. (d) The rf spectrum at the fourth harmonic with 1 GHz span.

According to the analysis in Ref. [12], the pulse-to-pulse energy fluctuations ΔE and the timing jitter Δt of the output pulse train can be evaluated through the analysis of the rf spectra. Our analysis suggests the excellent performance for the fourth HML ANDi fiber laser with low amplitude fluctuations (0.2%) and relatively low timing jitter (∼4 ps).

Finally, the fourth HML pulses from the laser cavity are externally compressed by using a pair of gratings of 600 lines/mm with an incidence angle of 27° under the pump power of 500 mW. Figure 9 shows the autocorrelation temporal pulse shape (black line) and the Sech^2 fitting (red dashed line) of the compressed pulses, which shows pulse duration of 627 fs. The mea-

sured maximum average power at the fourth harmonic is 110 mW, which corresponds to the pulse energy as high as 1.25 nJ.

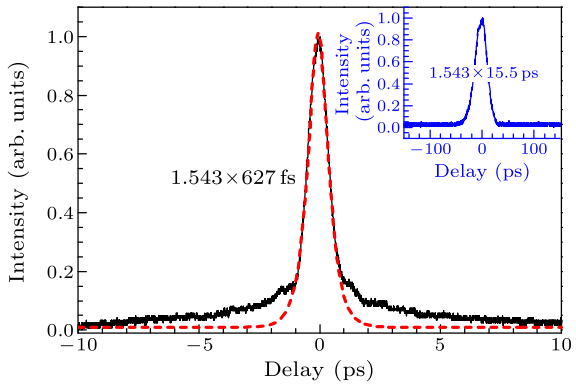

Fig. 9. Experimental (black line) and simulated (red dashed line) autocorrelation trace of the output compressed pulses. Inset: uncompressed autocorrelation trace of the output pulses for the ANDi laser operated at the fourth HML.

The main mechanism of the HML Yb-doped ANDi fiber laser can be explained by detuning of the frequency of the narrow-band birefringent filter relative to the center frequency of the gain spectrum.[13,14] Based on our experimentally observed results, the slightly detuning frequency introduced by the birefringent filter changes the original phase relationship of the fundamental mode-locking, and new mode-locked regime can be established, in which the phases between soliton bunches which contain multiple pulse are the same or with differences of $2n\pi$ (n is an integer), while the phase and the relative velocity (δv) between interpulses in a dissipative soliton bunch can be changed. By assisted adjustment of waveplates which introduce a phase offset, the soliton bunch state can be broken and eventually evolved into the in-phase constant speed HML state. In addition, the realization of high-order harmonic mode-locking with high peak signal-to-noise ratio is also believed to be connected to the total dispersion of the cavity and the effective spectral filter bandwidth, which can be controlled through the optimization and selection of parameters.

In conclusion, the nonlinear polarization evolution-based stable fourth harmonic mode-locked Yb ANDi fiber laser with 73 dB high peak signal-to-noise ratio at a repetition rate of 88 MHz is obtained. The average output power is 110 mW with ∼1.25 nJ pulse energy and compressed pulse duration of 627 fs. When the harmonic mode-locking is weak, soliton bunches which contain multipulses are generated by adjustment of the combination of the waveplates and the narrow-band birefringent filter. The demonstration of the soliton bunch with controllable pulse separation and numbers in ANDi fiber laser can extend our understanding for dissipative soliton mode-locking and the fiber laser will have a wide range of applications such as optical comb and coherent synthesizer.

References

[1] Wang G Z, Meng F, Li C, Jiang T X, Wang A M, Fang Z J and Zhang Z G 2014 *Opt. Lett.* **39** 2534
[2] Grudinin A B, Richardson D J and Payne D N 1993 *Electron. Lett.* **29** 1860
[3] Hsiang W W, Lin C Y, Tien M F and Lai Y C 2005 *Opt. Lett.* **30** 2493
[4] Zhang Z X, Zhan L, Yang X X, Luo S Y and Xia Y X 2007 *Laser Phys. Lett.* **4** 592
[5] Lecaplain C and Grelu P 2013 *Opt. Express* **21** 10897
[6] Usechak N G and Agrawal G P 2004 *Opt. Lett.* **29** 1360
[7] Zhou S, Ouzounov D G and Wise F W 2006 *Opt. Lett.* **31** 1041
[8] Kong L J, Xiao X S and Yang C X 2011 *Chin. Phys.* B **20** 024207
[9] Wang J L, Bu X B, Wang R, Zhang L, Zhu J F, Teng H, Han H N and Wei Z Y 2014 *Appl. Opt.* **53** 5088
[10] Gao J, Ge T W and Wang Z Y 2014 *Opt. Eng.* **53** 086109
[11] Zhu X J, Wang C H, Liu S X and Zhang G J 2012 *IEEE Photon. Technol. Lett.* **24** 754
[12] Zhang M, Kelleher E J R, Torrisi F, Sun Z, Hasan T, Popa D, Wang F, Ferrari A C, Popov S V and Taylor J R 2012 *Opt. Express* **20** 25077
[13] Komarov A, Komarov K, Leblond H and Sanchez F 2007 *J. Opt. A: Pure Appl. Opt.* **9** 1149
[14] Chong C Y 2008 *PhD Dissertation* (New York: Cornell University)